

Proteinase-3-antineutrophil cytoplasmic antibody-associated vasculitis secondary to subacute infective endocarditis: A case report

HUI LU¹⁻⁵, ZHAO CUI¹⁻⁵, XU-JIE ZHOU¹⁻⁵, YING YANG⁶, XIAO-NING HAN⁶,
XI-HUI LI⁷, FU-DE ZHOU¹⁻⁵ and MING-HUI ZHAO¹⁻⁵

¹Renal Division, Department of Medicine, Peking University First Hospital; ²Institute of Nephrology, Peking University; ³Key Laboratory of Renal Disease, Ministry of Health of China; ⁴Key Laboratory of Chronic Kidney Disease Prevention and Treatment, Ministry of Education of China; ⁵Research Units of Diagnosis and Treatment of Immune-mediated Kidney Diseases, Chinese Academy of Medical Sciences; Departments of ⁶Cardiology and ⁷Cardiac Surgery, Peking University First Hospital, Beijing 100034, P.R. China

Received June 10, 2023; Accepted February 2, 2024

DOI: 10.3892/etm.2024.12504

Abstract. A 58-year-old male patient was admitted to Peking University First Hospital (Beijing, China) due to recurrent hematuria, proteinuria and kidney dysfunction. The patient was positive for proteinase-3 (PR3)-antineutrophil cytoplasmic antibody (ANCA). Pathology of the kidney showed focal proliferative necrotizing glomerulonephritis with crescent formation and immune complex-mediated glomerulonephritis. The patient was diagnosed with PR3-ANCA-associated vasculitis (AAV), received intensive immunosuppressive therapy and experienced two relapses within 1 year. After admission, aortic valve vegetation was observed via echocardiography. The patient subsequently received antibiotic treatment and valve replacement, and achieved complete remission of kidney and cardiac function. The present case emphasized the importance of identifying secondary reasons for ANCA formation, especially infective endocarditis in patients with PR3-AAV.

Introduction

Antineutrophil cytoplasmic antibody (ANCA)-associated vasculitis (AAV) is a group of autoimmune diseases characterized by necrotizing vasculitis of small vessels, including microscopic polyangiitis, granulomatosis with polyangiitis and eosinophilic granulomatosis with polyangiitis; for these diseases, ANCAs targeting proteinase-3 (PR3) or myeloperoxidase are important diagnostic markers (1,2).

ANCA can also be detected in some patients with infectious diseases such as subacute infective endocarditis, human immunodeficiency virus (HIV) infection, chronic hepatitis B virus infection and tuberculosis (3-6). It is crucial to distinguish infections from AAV, as they have completely different treatments and immunosuppressive drugs for primary vasculitis can worsen infectious diseases (6).

The present study reports a patient who presented with rapidly progressive glomerulonephritis (RPGN) due to PR3-AAV. The patient experienced two relapses of acute kidney injury and was ultimately diagnosed with subacute infective endocarditis after 1 year. Valve replacement surgery and antibiotic treatment achieved complete remission of both kidney and cardiac function.

With the current case, the present study aimed to emphasize the importance of identifying the causes of secondary AAV to improve the understanding of the disease by clinicians, preventing misdiagnosis and missed diagnosis, and providing experience for its clinical diagnosis and treatment.

Case report

A 58-year-old male patient who had a history of hypertension for 6 years was admitted to Peking University First Hospital (Beijing, China) in December 2017 due to hematuria, proteinuria and kidney dysfunction for 1 year and dyspnea for 2 weeks.

The patient presented with fatigue and anorexia 1 year beforehand (August 2016). Urinalysis revealed 50-70 deformed red blood cells (normal range, 0-3) per high-power field. Urinary protein excretion was 0.51 (normal range, <0.15) g/day and the serum albumin concentration was 33.2 (normal range, 40-55) g/l. The serum creatinine (SCr) concentration was 209 (normal range, 44-133) μ mol/l. The white blood cell count of the patient was 6.2 (normal range, 3.5-9.5) $\times 10^9$ /l and the neutrophil count was 3.6 (normal range, 1.8-6.3) $\times 10^9$ /l. C-reactive protein (CRP) was 13.4 (normal range, 0-8) mg/l, and the erythrocyte sedimentation rate (ESR) was

Correspondence to: Professor Zhao Cui, Renal Division, Department of Medicine, Peking University First Hospital, 8 Xishiku Street, Xicheng, Beijing 100034, P.R. China
E-mail: cuizhao@bjmu.edu.cn

Key words: antineutrophil cytoplasmic antibody, proteinase-3, vasculitis, infective endocarditis, valve vegetation

60 (normal range, 0-15) mm/h. The serum c-ANCA concentration was 1:32 (serum:diluent; normal range, negative), and the anti-PR3 antibody concentration was >200 (normal range, <20) RU/ml. The rheumatoid factor (RF) concentration was 155 (normal range, <30) IU/ml, and the circulating immune complex (CIC) concentration was 147.1 (normal range, <20) RU/ml. The IgG concentration was 35.1 (normal range, 7.2-16.8) g/l, and the complement C3 concentration was 0.507 (normal range, 0.6-1.5) g/l. Antinuclear antibody (IIF) and anti-glomerular basement membrane (GBM) antibody were negative. Hepatitis B, hepatitis C, syphilis and HIV screening were negative. Kidney pathology revealed focal proliferative necrotizing glomerulonephritis accompanied by crescent formation and immune complex-mediated glomerulonephritis (Fig. 1A). Immunofluorescence staining of frozen tissues was performed to detect IgG (Fig. 1Aa) and C3 (Fig. 1Ab), and was evaluated under a fluorescence microscope as described previously (7). Kidney biopsy specimens were fixed in 4% buffered formaldehyde at 4°C for at least 4 h for light microscopy as described previously (8). Paraffin-embedded kidney sections (3 μ m) were used for histologic staining, including periodic acid-silver methenamine and Masson trichrome staining (Fig. 1Ac) and periodic acid-Schiff staining (Fig. 1Ad) as described previously (7). Approximately 1 cm³ of cortical renal tissue was taken, fixed with 3% glutaraldehyde, postfixed in 1% osmium acid, dehydrated with a graded acetone series and then embedded in epoxy resin. Tissues were then sliced into 80-nm ultrathin sections and analyzed using the JEM-1400 transmission electron microscope (Fig. 1Ae and Af) as described previously (9). Echocardiography revealed no vegetation (Fig. 2A). The patient was treated with a methylprednisolone pulse (500 mg/d x 3 days) two times, followed by prednisone 50 mg/d for ~1 month, combined with intravenous cyclophosphamide 0.6 g/month six times. After 1 month, the SCr concentration decreased to 136 μ mol/l, anti-PR3 antibody level decreased to 154 RU/ml and the general condition of the patient improved, with a Barthel activities of daily living (ADL) index score of 100 (10). Prednisone was gradually reduced to 20 mg/d and cyclophosphamide accumulated 3.6 g.

In March 2017, the patient had experienced recurrent fatigue, anorexia and gross hematuria. Urinary protein excretion was 2.4 g/d. SCr increased from 141 to 328 μ mol/l. The hemoglobin level of the patient decreased from 104 to 82 (normal range, 130-175) g/l, CRP level rose from 3 to 12 mg/l and ESR was 65 mm/h. The white blood cell count was 6.3x10⁹/l, and the neutrophil count was 5.1x10⁹/l. The anti-PR3 antibody concentration was 156 RU/ml. The patient was positive for cryoglobulin, monoclonal IgM λ and polyclonal IgG. RF was 50 IU/ml. C3 was 0.141 g/l and C4 was 0.103 (normal range, 0.12-0.36) g/l. No obvious abnormalities were found in the bone marrow. Echocardiography also revealed no vegetation. Kidney pathology was repeated and revealed AAV-associated kidney injury and proliferative glomerulonephritis (Fig. 1B). Kidney biopsy specimens were fixed in 4% buffered formaldehyde at 4°C for at least 4 h for light microscopy as described previously (8). Paraffin-embedded kidney sections (3 μ m) were used for histologic staining, including periodic acid-silver methenamine and Masson trichrome staining (Fig. 1Ba) and Masson trichrome staining (Fig. 1Bb) as described previously (7). Approximately 1 cm³

of cortical renal tissue was taken, fixed with 3% glutaraldehyde, postfixed in 1% osmium acid, dehydrated with a graded acetone series and then embedded in epoxy resin. Tissues were then sliced into 80-nm ultrathin sections and analyzed using the JEM-1400 transmission electron microscope (Fig. 1Bc and Bd) as described previously (9). The patient received two rounds of methylprednisolone pulse therapy, 3 L of plasma exchange every other day for six cycles, and two rounds of intravenous rituximab for a total of 600 mg (one 100 mg and another 500 mg 2 weeks later). Subsequently, the SCr concentration of the patient decreased to 170 μ mol/l in May 2017 and then to 99 μ mol/l in August 2017. Cryoglobulin testing became negative. RF was 25 IU/ml. C3 was 0.678 g/l, and C4 was 0.211 g/l. The patient's hemoglobin rose to 114 g/l. The anti-PR3 antibody test was negative. The number of total B cells was <5/ μ l. The patient's general condition improved, the Barthel ADL index score of the patient was 100 and prednisone was decreased to 7.5 mg/d.

At 2 weeks prior to this admission in December 2017, the patient developed dyspnea, orthopnea, nausea, anorexia and gross hematuria. Urinary protein excretion was 0.27 g/d (urine volume, 150 ml). Urinalysis revealed 100 red blood cells and 80 white blood cells (normal range, 0-5) per high-power field. The patient's white blood cell count was 23.4x10⁹/l, the neutrophil count was 19.8x10⁹/l, the hemoglobin level was 108 g/l and the platelet count was 184 (normal range, 125-350) x10⁹/l. CRP was 20 mg/l. The procalcitonin (PCT) level of the patient was 4.03 (normal range, <0.05) ng/ml. Alanine aminotransferase was 645 (normal range, 9-50) U/l, aspartate aminotransferase was 705 (normal range, 15-40) U/l, albumin was 28.2 g/l and SCr was 191 μ mol/l, lactate dehydrogenase was 2,220 (normal range, 100-240) IU/l, cardiac troponin (CTnI) was 0.76 (normal range, 0-0.03) ng/ml and brain natriuretic peptide was 2,988 (normal range, <100) pg/ml. The patient was treated with 40 mg/d methylprednisolone and admitted to Peking University First Hospital (Beijing, China) in December 2017.

On admission, the body temperature of the patient was 36.5°C, his blood pressure was 90/60 mmHg and heart rate was 110 beats/min. The patient's body weight was 55 kg and BMI was 19 kg/m². The conjunctiva was pale. There was no distension in the jugular vein. The breathing sounds in both lower lungs were weak with wet rales. The left cardiac boundary was enlarged, and S3 and III/6 systolic murmurs were heard in the apical area. The liver was palpable 3 cm under the right rib. There was mild tenderness under the xiphoid process, without rebound pain, and shifting dullness was present. There was no edema in either lower limb.

The patient was positive for type II cryoglobulin. C3 was <0.058 g/l, C4 was <0.032 g/l and C1q was 116.5 (normal range, 159-223) mg/l. ANCA, antinuclear antibody (IIF), anti- β 2-glycoprotein 1 antibody (ELISA), anticardiolipin antibody (ELISA) and anti-GBM antibody were negative. The IgG, IgA and IgM levels were within the normal range. The ESR was 21 mm/h. Infection screening, which included bacteria, fungi and viruses and was performed on serology and specimens, including sputum, stool and urine, was negative. Due to the long-term use of steroids and immunosuppressants and the high leukocyte, neutrophil counts and PCT, the patient received 1.5 g of intravenous cefoperazone-sulbactam every 12 h. Blood culture (after intravenous cefoperazone-sulbactam

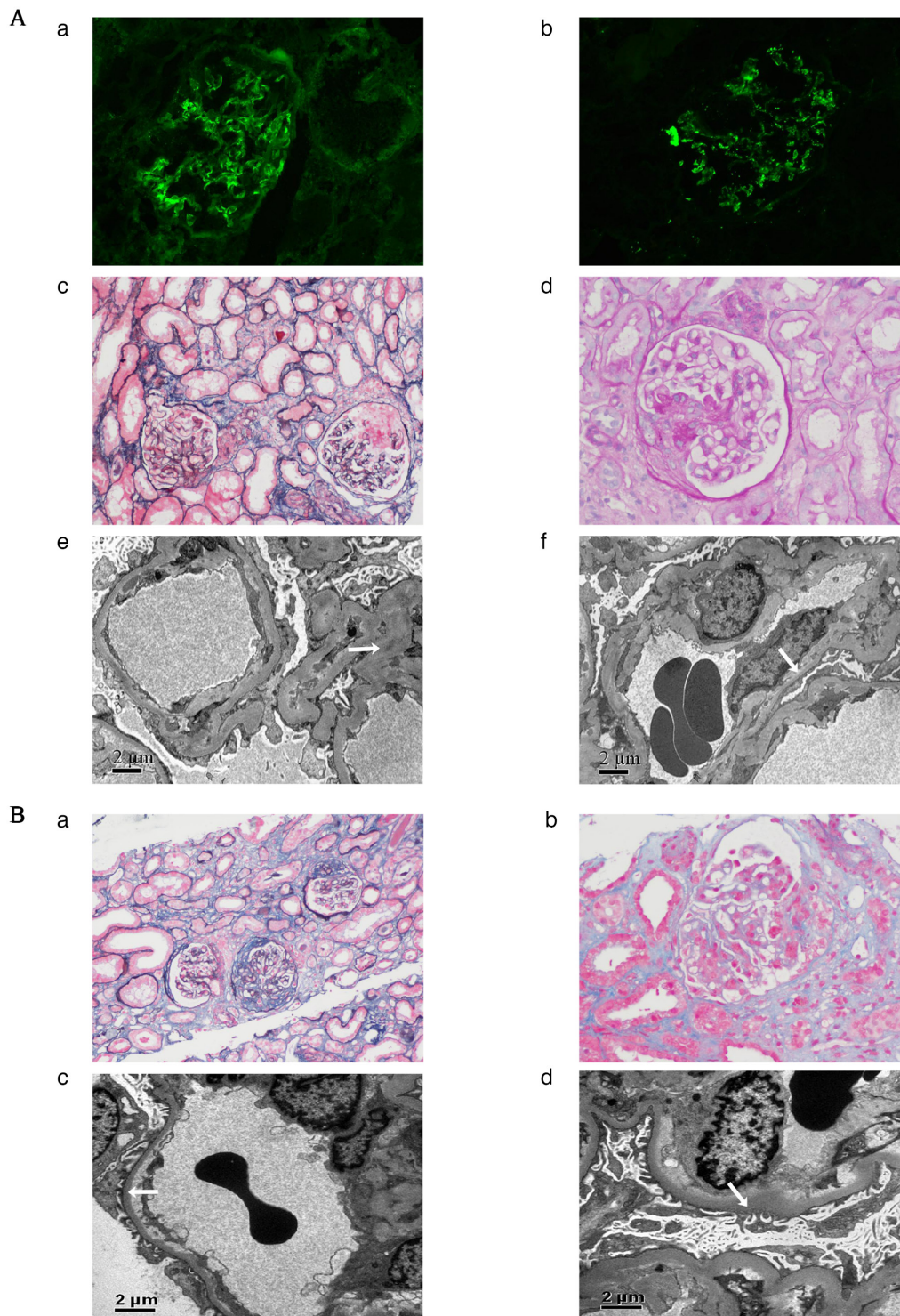


Figure 1. Kidney pathology of the patient. (A) At the first kidney pathology, immunofluorescence showed granular deposits of (Aa) IgG⁺⁺ (magnification, x200) and (Ab) C3⁺⁺⁺ (magnification, x200) in the mesangial area and along capillary walls. Light microscopy at a magnification of (Ac) x100 (periodic acid-silver methenamine and Masson trichrome staining) and (Ad) x200 (periodic acid-Schiff staining) showed serious damage to glomerular capillary loops, including four segmental fibrinoid necroses with small cellular crescents, two cellular crescents, 11 fibrocellular crescents, one fibrous crescent, four small fibrocellular crescents and six small fibrocellular crescents in a total of 59 glomeruli. The remaining 31 glomeruli showed mild segmental mesangial hypercellularity. The tubules presented with epithelial cell vacuolation, focal brush margin shedding and most of the erythrocytes were cast. Focal lymphoid and monocyte infiltration and a small amount of neutrophil infiltration were observed in the interstitium. Transmission electron microscopy (magnification, x8,000) showed (Ae) segmental endothelial cell proliferation, massive electron dense deposits in the mesangial area (arrow), (Af) segmental loose layer widening in the basement membrane and segmental fusion of the epithelial foot processes (arrow). (B) At the second kidney pathology, immunofluorescence showed granular deposits of IgM⁺⁺ and C3⁺⁺⁺ in the mesangial area. Light microscopy at a magnification of (Ba) x100 (periodic acid-silver methenamine and Masson trichrome staining) and (Bb) x200 (Masson trichrome staining) showed 24 glomeruli, including three fibrous crescents with sclerosis, one fibrocellular crescent and five small fibrocellular crescents. The remaining glomeruli showed slight diffuse hyperplasia of the mesangial cells and matrix, with focal segmental aggravation and fuchsinophilic deposition. Segmental endothelial cell proliferation. The tubules presented with epithelial cell vacuolation and granular degeneration, focal brush margin shedding and red blood cell and protein casts. The interstitium was focally infiltrated with lymphocytes and mononuclear cells. Transmission electron microscopy (magnification, x6,700) showed (Bc) no electronic dense deposits, (Bd) segmental loose layer widening in the basement membrane, and extensive fusion of the epithelial foot processes (arrow).

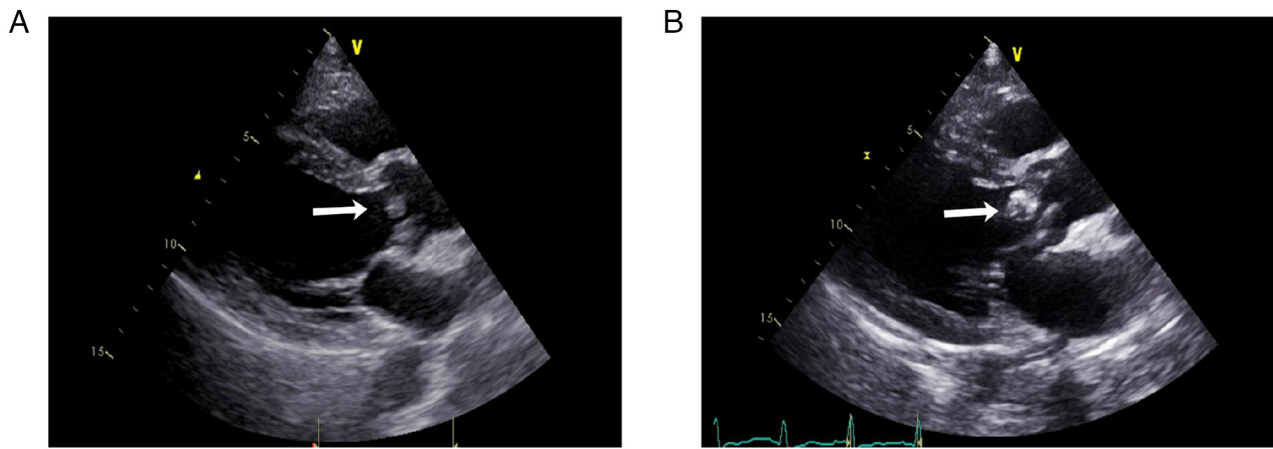


Figure 2. Cardiac ultrasonography of the patient. (A) At the time of disease onset, cardiac ultrasonography showed left ventricular symmetrical hypertrophy, moderate aortic regurgitation, aortic valve sclerosis/calcification (no aortic valve vegetation, arrow), mild aortic stenosis, mild mitral and tricuspid regurgitation and a normal left ventricular ejection fraction. (B) Approximately 1 year later, cardiac ultrasonography revealed aortic and mitral valve disorders, aortic valve vegetation (arrow), moderate to severe aortic regurgitation, mild aortic stenosis, severe mitral regurgitation, left atrium and left ventricular enlargement, left ventricular symmetrical hypertrophy, a normal left ventricular ejection fraction (62.3%), mild tricuspid regurgitation and elevated pulmonary systolic pressure.

at 1.5 g every 12 h for one week) was negative three times. Echocardiography (Fig. 2B) revealed vegetation on the aortic valve. The patient denied a history of intravenous illicit drug use. After careful questioning it was revealed that the patient had a history of tooth extraction without antibiotics 1 year prior.

The patient was diagnosed with PR3-AAV secondary to subacute infective endocarditis, accompanied by cryoglobulinemia. The patient received hemodialysis and was treated with intravenous cefoperazone-sulbactam at 1.5 g every 12 h for 1 month before surgery. The glucocorticoid was reduced to 10 mg/d. Mitral valve and aortic valve replacement and coronary artery bypass grafting were performed. Pathology revealed fibrous hyperplasia with calcification and tissue degeneration in the valve tissue, which was locally covered with endothelial cells. The vegetation culture test was also negative. Postoperatively, the patient continued to receive intravenous antibiotic treatment for 1 month, which included cefoperazone-sulbactam at 1.5 g every 12 h for 1 week, biapenem at 0.3 g every 12 h for 2 weeks and piperacillin-sulbactam at 2.5 g every 12 h for 1 week. At 1 week after surgery, echocardiography showed a normal left ventricular ejection fraction (55.5%), mild tricuspid regurgitation and mild pulmonary hypertension. After 3 weeks, the SCr level was normal. The patient's cardiac function recovered to Grade I (New York Heart Association grade) (11). Glucocorticoid and immunosuppressants were all stopped.

Discussion

The present study is a case of refractory PR3-AAV in which the patient experienced two relapses within 1 year under intensive glucocorticoid therapy, immunosuppressive therapy and plasma exchange. The features of cryoglobulinemia, hypocomplementemia and obvious cardiac insufficiency suggested secondary reasons for AAV, and echocardiography resulted in the diagnosis of aortic valve vegetation. Antibiotic treatment and valve replacement surgery (according to the guidelines of European Society of Cardiology and Chinese

Society of Cardiology) achieved complete remission of kidney and cardiac dysfunction in the absence of glucocorticoid and immunosuppressants. The present case demonstrated that identifying AAV driven by infections is of importance for preventing the exacerbation of infections caused by immunosuppressive drugs.

The differential diagnosis of secondary AAV from primary AAV can be challenging, especially for subacute infective endocarditis in which ~25% of the patients with RPGN are initially considered to have primary vasculitis (12). However, distinguishing AAV secondary to infection is highly valuable because of the entirely different therapies and outcomes used (12-14). In the present study, the patient was first diagnosed with primary PR3-AAV according to the 2012 Revised International Chapel Hill Consensus Conference Nomenclature of Vasculitides (1), based on crescent formation in the glomeruli, PR3-ANCA in the circulation and negative results from echocardiography and other screenings for malignancies or drugs. The patient received intensive treatment comprising steroids, immunosuppressants and plasma exchange, but experienced two relapses within 1 year.

There were several hints in the present case of PR3-AAV secondary to subacute infective endocarditis. i) Hypocomplementemia is not common in primary AAV (15). Although complement activation has been demonstrated to participate in the AAV mechanism (16) and therapies targeting C5 have achieved effectiveness in clinical trials (17), the circulating levels of C3 and C4 are mostly within the normal range in primary AAV (15). The reductions in C3 and C4, together with the increase in the circulating immune complex and in the amount of immune complex deposits in the glomeruli, prompted possible infections in the current patient. ii) Cryoglobulinemia is rare in primary AAV. Type II cryoglobulin was detected in the current patient, which is often due to chronic infections or malignancies (18). The bone marrow and lymph nodes were screened, and the results were negative. Hepatitis, syphilis, HIV and tuberculosis were also negative. Thus, subacute infective endocarditis was

suspected to be the cause of the patient's cryoglobulinemia. iii) Pericarditis, myocarditis and abnormal conduction have been reported in patients with cardiac involvement of primary AAV, but valve lesions are rare (19-22). According to the literature review by Chirinos *et al* (15), the most common echocardiographic findings of endocardial compromise in patients with AAV are aortic valve thickening and aortic insufficiency with or without aortic root dilatation. Thus, the presence of aortic valve vegetation in the present patient was suspected to indicate subacute infective endocarditis rather than cardiac involvement of the primary AAV. Blood culture was performed three times, and vegetation culture was performed after surgery; however, all the results were negative because of continuous antibiotic treatment during the disease course.

Kidney damage in patients with infective endocarditis is characterized by necrotizing and crescentic glomerulonephritis (53%) or endocapillary proliferative glomerulonephritis (37%). C3 deposition occurs in almost all patients, but IgG deposition is less common (<30%). Electron dense deposits can be observed in most patients via electron microscopy. In addition, 28% of the patients are ANCA positive. Most of them are PR3-ANCA and may be depleted after the resolution of infective endocarditis. A total of 56% of the patients are complicated with hypocomplementemia and some are also cryoglobulin positive (15,23-25). These features were also revealed in the present case.

The pathogenesis of ANCA formation in infective endocarditis is not clear. Mahr *et al* (26) reported that among patients with infective endocarditis, ANCA-positive patients had echocardiography-documented vegetation more often than ANCA-negative patients did. The antigenic stimulation by neutrophilic enzymes released within vegetation and the non-specific hyperimmune humoral response may be the underlying mechanisms. Konstantinov *et al* (27) discussed the proposed mechanisms of ANCA formation during the course of infections, including autoantigen complementarity, molecular mimicry between bacteria and self-antigens, epigenetic modifications, neutrophil extracellular traps and interactions between bacterial components and Toll-like receptors. Further investigations are required to clarify these mechanisms to further develop preventive measures and therapeutic interventions.

In conclusion, the present study reported a case of PR3-AAV secondary to infective endocarditis, which highlighted the necessity of identifying the causes of ANCA formation, including infections, drugs, malignancies and others, not only at the first diagnosis but also during the disease course.

Acknowledgements

Not applicable.

Funding

This work was supported by grants from the Natural Science Foundation of China (grant nos. 81870486, 82070732 and 82090021) and CAMS Innovation Fund for Medical Sciences (grant no. 2019-I2M-5-046).

Availability of data and materials

The data generated in the present study may be requested from the corresponding author.

Authors' contributions

HL and ZC collected and analyzed the patient data and wrote the manuscript. XJZ and XNH obtained echocardiography images. ZC, XJZ, YY, XNH, XHL and FDZ advised on patient treatment. MHZ advised on patient treatment and gave approval of the manuscript to be published. HL and ZC confirm the authenticity of all the raw data. All authors read and approved the final manuscript.

Ethics approval and consent to participate

The study followed the Declaration of Helsinki and was approved by the ethics committee of Peking University First Hospital [approval no. 2017 (1280)].

Patient consent for publication

Written informed consent was obtained from the patient for publication of the data and images in this case report.

Competing interests

The authors declare that they have no competing interests.

References

- Jennette JC, Falk RJ, Bacon PA, Basu N, Cid MC, Ferrario F, Flores-Suarez LF, Gross WL, Guillevin L, Hagen EC, *et al*: 2012 revised international chapel hill consensus conference nomenclature of vasculitides. *Arthritis Rheum* 65: 1-11, 2013.
- Bosch X, Guilabert A and Font J: Antineutrophil cytoplasmic antibodies. *Lancet* 368: 404-418, 2006.
- Uh M, McCormick IA and Kelsall JT: Positive cytoplasmic antineutrophil cytoplasmic antigen with PR3 specificity glomerulonephritis in a patient with subacute bacterial endocarditis. *J Rheumatol* 38: 1527-1528, 2011.
- Mandell BF and Calabrese LH: Infections and systemic vasculitis. *Curr Opin Rheumatol* 10: 51-57, 1998.
- Fukasawa H, Hayashi M, Kinoshita N, Ishigaki S, Isobe S, Sakao Y, Kato A, Fujigaki Y and Furuya R: Rapidly progressive glomerulonephritis associated with PR3-ANCA positive subacute bacterial endocarditis. *Intern Med* 51: 2587-2590, 2012.
- Ying CM, Yao DT, Ding HH and Yang CD: Infective endocarditis with antineutrophil cytoplasmic antibody: Report of 13 cases and literature review. *PLoS One* 9: e89777, 2014.
- Xing GQ, Chen M, Liu G, Wang SX and Zhao MH: Renal neutrophils infiltration in antineutrophil cytoplasmic antibodies-negative pauci-immune crescentic glomerulonephritis. *Am J Med Sci* 340: 474-480, 2010.
- Yong ZH, Yu XJ, Liu JX, Zhou FD, Wang SX and Zhao MH: Kidney histopathologic spectrum and clinical indicators associated with MGRS. *Clin J Am Soc Nephrol* 17: 527-534, 2022.
- Yuan X, Su Q, Wang H, Shi S, Liu L, Lv J, Wang S, Zhu L and Zhang H: Genetic variants of the COL4A3, COL4A4, and COL4A5 genes contribute to thinned glomerular basement membrane lesions in sporadic IgA nephropathy patients. *J Am Soc Nephrol* 34: 132-144, 2023.
- Liu W, Unick J, Galik E and Resnick B: Barthel Index of activities of daily living: Item response theory analysis of ratings for long-term care residents. *Nurs Res* 64: 88-99, 2015.

11. McDonagh TA, Metra M, Adamo M, Gardner RS, Baumbach A, Böhm M, Burri H, Butler J, Čelutkienė J, Chioncel O, *et al*: 2021 ESC Guidelines for the diagnosis and treatment of acute and chronic heart failure. *Eur Heart J* 42: 3599-3726, 2021.
12. Ai S, Liu J, Ma G, Ye W, Hu R, Zhang S, Fan X, Liu B, Miao Q, Qin Y and Li X: Endocarditis-associated rapidly progressive glomerulonephritis mimicking vasculitis: A diagnostic and treatment challenge. *Ann Med* 54: 754-763, 2022.
13. Brunet A, Julien G, Cros A, Beaudoux O, Hittinger-Roux A, Bani-Sadr F, Servettaz A and N'Guyen Y: Vasculitides and glomerulonephritis associated with *Staphylococcus aureus* infective endocarditis: Cases reports and mini-review of the literature. *Ann Med* 52: 265-274, 2020.
14. Satoskar AA, Parikh SV and Nadasdy T: Epidemiology, pathogenesis, treatment and outcomes of infection-associated glomerulonephritis. *Nat Rev Nephrol* 16: 32-50, 2020.
15. Chirinos JA, Corrales-Medina VF, Garcia S, Lichtstein DM, Bisno AL and Chakko S: Endocarditis associated with antineutrophil cytoplasmic antibodies: A case report and review of the literature. *Clin Rheumatol* 26: 590-595, 2007.
16. Chen M, Jayne DRW and Zhao MH: Complement in ANCA-associated vasculitis: Mechanisms and implications for management. *Nat Rev Nephrol* 13: 359-367, 2017.
17. Jayne DRW, Merkel PA, Schall TJ and Bekker P; ADVOCATE Study Group: Avacopan for the treatment of ANCA-associated vasculitis. *N Engl J Med* 384: 599-609, 2021.
18. Silva F, Pinto C, Barbosa A, Borges T, Dias C and Almeida J: New insights in cryoglobulinemic vasculitis. *J Autoimmun* 105: 102313, 2019.
19. Hagen EC, Daha MR, Hermans J, Andrassy K, Csernok E, Gaskin G, Lesavre P, Lüdemann J, Rasmussen N, Sinico RA, *et al*: Diagnostic value of standardized assays for anti-neutrophil cytoplasmic antibodies in idiopathic systemic vasculitis. EC/BCR project for ANCA assay standardization. *Kidney Int* 53: 743-753, 1998.
20. Goodfield NE, Bhandari S, Plant WD, Morley-Davies A and Sutherland GR: Cardiac involvement in Wegener's granulomatosis. *Br Heart J* 73: 110-115, 1995.
21. Bourgarit A, Toumelin PL, Pagnoux C, Cohen P, Mahr A, Guern VL, Mouthon L and Guillevin L; French Vasculitis Study Group: Deaths occurring during the first year after treatment onset for polyarteritis nodosa, microscopic polyangiitis, and Churg-Strauss syndrome: A retrospective analysis of causes and factors predictive of mortality based on 595 patients. *Medicine (Baltimore)* 84: 323-330, 2005.
22. Lacoste C, Mansencal N, Ben M'rad M, Goulon-Goeau C, Cohen P, Guillevin L and Hanslik T: Valvular involvement in ANCA-associated systemic vasculitis: A case report and literature review. *BMC Musculoskelet Disord* 12: 50, 2011.
23. Choi HK, Lamprecht P, Niles JL, Gross WL and Merkel PA: Subacute bacterial endocarditis with positive cytoplasmic antineutrophil cytoplasmic antibodies and anti-proteinase 3 antibodies. *Arthritis Rheum* 43: 226-231, 2000.
24. Bonaci-Nikolic B, Andrejevic S, Pavlovic M, Dimcic Z, Ivanovic B and Nikolic M: Prolonged infections associated with antineutrophil cytoplasmic antibodies specific to proteinase 3 and myeloperoxidase: Diagnostic and therapeutic challenge. *Clin Rheumatol* 29: 893-904, 2010.
25. Boils CL, Nasr SH, Walker PD, Couser WG and Larsen CP: Update on endocarditis-associated glomerulonephritis. *Kidney Int* 87: 1241-1249, 2015.
26. Mahr A, Batteux F, Tubiana S, Goulvestre C, Wolff M, Papo T, Vrtovsnik F, Klein I, Jung B and Duval X; IMAGE Study Group: Brief report: Prevalence of antineutrophil cytoplasmic antibodies in infective endocarditis. *Arthritis Rheumatol* 66: 1672-1677, 2014.
27. Konstantinov KN, Ulf-Møller CJ and Tzamaloukas AH: Infections and antineutrophil cytoplasmic antibodies: Triggering mechanisms. *Autoimmun Rev* 14: 201-203, 2015.



Copyright © 2024 Lu *et al*. This work is licensed under a Creative Commons Attribution-NonCommercial-NoDerivatives 4.0 International (CC BY-NC-ND 4.0) License.